Effect of Feed Rate and Impact Angle on the Erosive Wear of High Velocity Oxy-fuel Sprayed Coating Under High Temperature Conditions

SATPAL SHARMA

School of Engineering, Gautam Buddha University, Greater Noida, U. P. (India)

Abstract — In the present investigation erosive wear behavior of EWAC 1006 Co-base alloy deposited by high velocity oxy-fuel (HVOF) spraying process was investigated. The microstructure, porosity and hardness of the coating was evaluated. The effect of impact angles of 30°, 60° and 90° and erodent feed rate of 1, 3, 5 g/min on the erosive wear were evaluated. All erosive wear tests were conducted at high temperature (450°C) against erodent velocity of 40 m/s. The erosive wear was found to decrease with the increase in impact angle of the erodent and increase with the increase in erodent feed rate. The erosive wear of the coating was 3-4 times lower than the substrate. Analysis of the scanning electron microscope images revealed cutting and lip formation as the material removal mechanisms in these coatings under erosive wear conditions used in this investigation.

INTRODUCTION

Erosion is a serious problem in many engineering systems, including steam and jet turbines, pipelines and valves used in slurry transportation of matter, and fluidized bed combustion systems [1, 2]. A Co-base alloy with an appropriate composition is widely selected for different types of wear applications. This alloy exhibit good wear and corrosion resistance even up to 750°C [3–5].

Hejwowski et al. [6] studied the erosive wear behavior of flame sprayed NiCrSiB hard surfacing alloys and found that the NiCrSiB offered a better wear resistance as compared to steel. Hoop et al. [7] studied the high temperature erosion

---

*Author for correspondence. E-mail : satpal78sharma@gmail.com

behavior of thermal sprayed metallic and cermet coatings (WC, Ni and Co-based) on boiler tube materials by using silica as erodent and reported that the coatings containing large quantities of defects (particularly porosity) did not provide good erosion resistance. It was suggested that to provide good erosion resistance, coatings must have fine and homogeneous structures.

Hawthorne et al. [8] studied the performance of 10 high velocity oxy-fuel (HVOF) sprayed coatings under both solid particle and slurry erosion conditions at 20° and 90° impact angles. Ranking of various coatings in solid particle erosion were (WC-12Co) < {WC-12Co-50wt.% (NiCrBSiFe)} < (Cr$_3$C$_2$-25wt.%NiCr) < (CoCrNiMoWFe) < (NiWCrSiFeBC). Mishra et al. [9] conducted erosion studies using an air-jet erosion test rig at a velocity of 40 m/s and impingement angles of 30° and 90° on uncoated Co-based superalloy (3Fe–10Ni–20Cr–1.5Mn–0.3Si–0.08C–15W–Balance Co) as well as plasma sprayed NiCrAlY, Ni–20Cr and Ni$_3$Al-coated superalloy specimens at room temperature. Ni$_3$Al coating showed the least erosion rate at 90° impact angle, whereas the NiCrAlY coating showed the lowest erosion rate at 30° impact angle. The Ni–20Cr coating showed the highest erosion rate with both the impact angles. The bare cobalt-based super alloy showed better erosion resistance as compared to the plasma-sprayed coatings.

Stein et al. [10] studied the solid particle erosion of cermet (FeCrAlY–CrC and NiCr–CrC) coatings deposited by high velocity oxy-fuel (HVOF) process. It was found that decreasing the carbide and oxide content, decreased the erosion rate for 90° impact angles while for 30° impact angle the erosion rate remained fairly constant regardless of carbide and hard phase content. Vicenzi et al. [11] investigated WC–12Co, Cr$_3$C$_2$–NiCr and WC–CrC–Ni thermal sprayed coatings produced by the high velocity oxygen fuel (HVOF) spraying process under high temperature (310°C). Investigations showed that WC-12Co, Cr$_3$C$_2$-NiCr, and WC-CrC-Ni offered higher erosion resistance than bare 1020 steel. WC-12Co coating worn about 18 times less than bare steel, followed by WC-CrC-Ni and Cr$_3$C$_2$-NiCr coatings worn 13 and 9 times less respectively. Solid particle erosion behavior of the HVOF deposited NiCr and Stellite-6, coatings on boiler tube steels (GrA1) was evaluated using an air jet erosion test rig at a velocity of 26 m/s and impingement angle of 30° and 90° on uncoated as well as HVOF spray coated boiler tube steels at 250°C. It was reported that the NiCr coating performed better than Stellite-6 coating during solid particle erosion for both impact angles [12]. The literature review discussed above shows that a small amount of work was carried out considering the effect of erodent feed rate and impact angle. In view of the above facts, the aim of the present investigation was to study the effect of impact angle and erodent feed rate under high temperature condition on the erosion wear of HVOF sprayed Co-base coatings.

EXPERIMENTAL PROCEDURE

Materials and methods :

The carbon steel substrate was used for HVOF coating deposition. The substrate was degreased and roughened to an average surface roughness of Ra 3.15 μm (Rmax 18.2 μm). The normal composition of substrate and commercially available Co-base powder is shown in Table 1. The powder coatings were deposited by high velocity oxy-fuel (HVOF) spraying process. High velocity oxy-fuel coatings were deposited using the

TABLE 1.

Chemical composition (wt %) of substrate and surfacing powder

Elements / Material	C	Ni	Cr	W	Si	Fe	Co	Mn
M.S. Substrate	0.2–0.22	–	–	–	0.4–0.6	Bal.	–	0.4–0.8
Co-base powder	3.0–3.5	20–25	28–30	5–6	0.2–0.5	–	Bal.	0.5–0.7

Sulzer Metco DJ 2600 system at VA- Tech Escher Wyss Flovel Ltd., Faridabad (Haryana), India. The HVOF spraying parameters for the development of 1006 coating powders are shown in Table 2. The substrate was preheated to $200\pm10°C$.

Characterization of coating :

Coated samples were cut transversely for microstructural characterization (SEM- LEO –435- VP, England), porosity and hardness. The samples were polished using standard metallographic procedure and etched with a chemical mixture of 3 parts HCl + 1 part HNO_3. SEM micrographs were used to study microstructure and worn surfaces. The porosity was measured by the point counting method [13, 14]. The average of 25 areas of each coating has been used for porosity measurement. Vickers microhardness of the coating was measured using a load of 100 g and average of ten readings of the coating hardness was used in the study. Scanning electron microscopy of the worn surfaces of coatings was also carried out to identify the material removal mechanisms under erosive wear conditions.

Erosive wear test :

High temperature erosive wear behavior of HVOF sprayed coatings was studied using high temperature erosion tester. The HVOF spray coated samples were cut into sizes of 16 × 15 × 5 mm^3 for erosive wear testing. The samples were polished to 1-2

TABLE 2.

Process parameters used for development of HVOF coatings

Spraying parameter	Parameter setting
Pressure – Oxygen (MPa)	0.081
Flow – Oxygen (l/min)	32
Pressure – Hydrogen (MPa)	0.066
Hydrogen – Oxygen (l/min)	62
Pressure – Air (MPa)	0.051
Flow – Air (l/min)	44
Pressure – Carrier gas – Nitrogen (MPa)	0.069
Flow – Carrier gas – Nitrogen (l/min)	44
Powder flow (g/min)	50
Spraying distance (mm)	250
Traverse speed of gun (mm/s)	550
Maximum surface temperature during spraying °C	90

μm surface roughness (Ra) in order to obtain identical surface conditions on all erosive wear samples. The sample were cleaned with acetone, dried and weighed to an accuracy of 0.0001 g before erosive wear test. The air pressures and frequencies corresponding to velocity and erodent feed rate are shown in Table 3. Al_2O_3 of 50 μm size was used as an erodent. An electronic balance (accuracy 0.0001 g) was used for weighing the samples after washing in acetone before and after erosive wear test. The weight loss was used as a measure of erosive wear.

TABLE 3.

Relation between (a) air pressure and velocity and (b) frequency and feed rate used for setting the parameters (factors) in erosive wear test

(a)		(b)	
Air pressure, kg/cm^2	Velocity, m/s	Frequency, Hz	Feed rate, g/min.
0.7	30	1.1	1
1.1	45	5	3
1.75	60	8.1	5

RESULTS AND DISCUSSIONS

Microstructure :

The metallographic characterization of 1006 Co-base powder coating was carried out using backscattered electron (BSE) micrographs as shown in Fig. 1. In BSE micrographs the contrast is related to the atomic number of the elements present. The phases containing lower atomic number elements, like oxides, appear dark in SEM
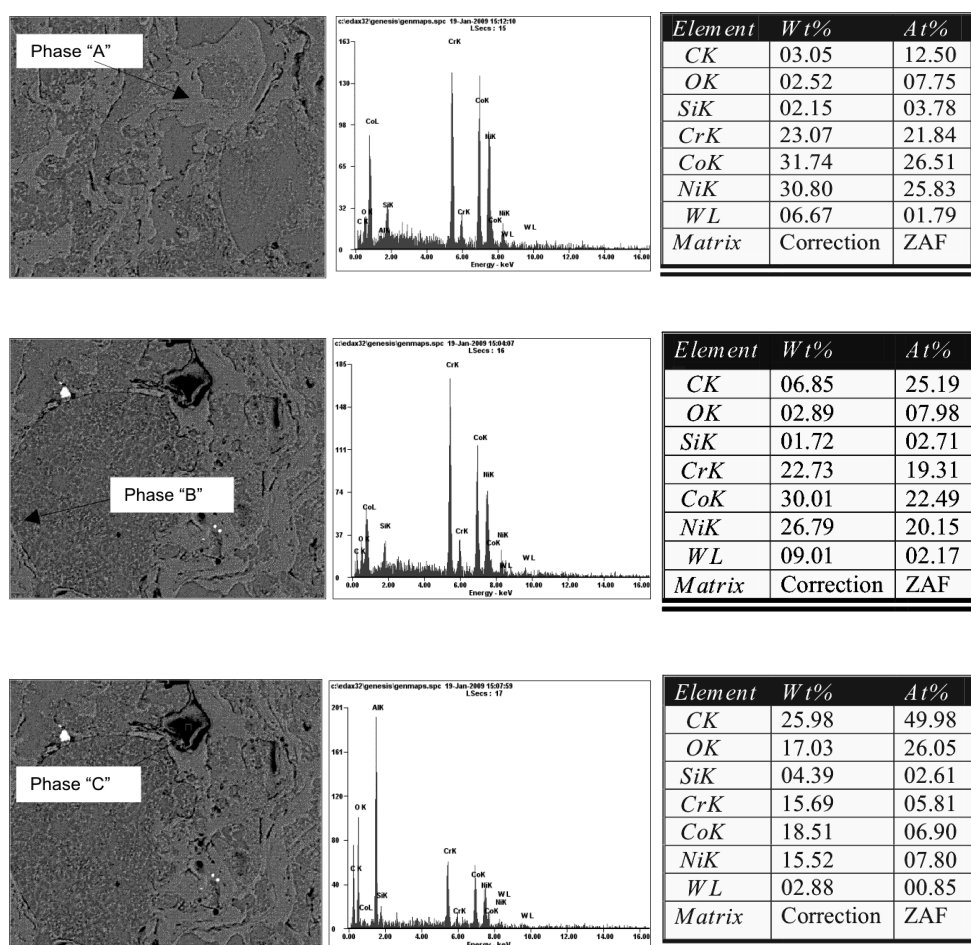

Element	Wt%	At%
CK	03.05	12.50
OK	02.52	07.75
SiK	02.15	03.78
CrK	23.07	21.84
CoK	31.74	26.51
NiK	30.80	25.83
WL	06.67	01.79
Matrix	Correction	ZAF

Element	Wt%	At%
CK	06.85	25.19
OK	02.89	07.98
SiK	01.72	02.71
CrK	22.73	19.31
CoK	30.01	22.49
NiK	26.79	20.15
WL	09.01	02.17
Matrix	Correction	ZAF

Element	Wt%	At%
CK	25.98	49.98
OK	17.03	26.05
SiK	04.39	02.61
CrK	15.69	05.81
CoK	18.51	06.90
NiK	15.52	07.80
WL	02.88	00.85
Matrix	Correction	ZAF

Fig. 1. Microstructure of 1006 Co-base powder coating – phase "A", phase "B" and phase "C", their corresponding EDAX and wt.% of elements distribution in coating deposited by HVOF.

micrographs, however, in some cases carbide particles also appear dark in SEM micrographs as reported by Shetty et al. [15]. Various constituents of thermal-spray coatings such as matrix phase, carbides, oxides and porosity, can be identified by the differences in contrast of different phases [16].

In this investigation BSE micrographs of 1006 Co-base coatings have been used for microstructural study.Three different phases namely phase "A", "B" and "C" were identified by the EDAX analysis of the coating. The phases "A" and "B" contain almost same wt%. of Co and Cr, while phase "A" contains higher wt%. of Ni as compared to phase "B". The phase "B" contains higher wt%. of W as compared to phase "A". The phase "C" is rich in C along with O, Cr, Ni and Co.

Porosity and Microhardness :

The microstructure formed in the 1006 Co-base powder coatings developed by HVOF process are rather dense. The low porosity in these coatings is primarily attributed to the higher particle velocity, relatively low temperature (3000°C) (as compared to vacuum plasma (12000°C) and detonation gun (4000°C)) [17] and higher impact velocity of the powder particles on the substrate material. The porosity (%) in 1006 Co-base powder coating was found as 1.52 %.

The overall average microhardness of 1006 coating was found to be 735 ± 135 $Hv_{0.1}$. Vite et al. [18] also reported the Vicker's hardness of such type of alloys as $757Hv_{0.049}$. The high hardness of this type of alloy has been reported due to solid solution hardening by W, Cr and carbides [19]. The non-uniformity in microhardness of the coatings is attributed to the microstructural inhomogeneity in these coatings in the form of porosity; oxidized, unmelted and semi-melted particles in the coating.

Erosion behavior :

All erosive wear tests were conducted at 450°C against velocity of 40 m/s. The erosive wear behavior of substrate and HVOF sprayed coating as a function of impact angle and feed rate of erodent are shown graphically in Fig. 2 (a-b). There is decrease in erosive wear with the increase in impact angle as can be observed from Fig. 2 (a). This is due to ductile behavior of the various constituents of the coating material. At low impact angle the material removal is known to take place mainly by cutting mechanism while at high impact angles the material removal mainly takes place through lip formation which is caused due to deformation. Due to repeated impacts of the erodent strain hardening of lips takes place and subsequently these lips as
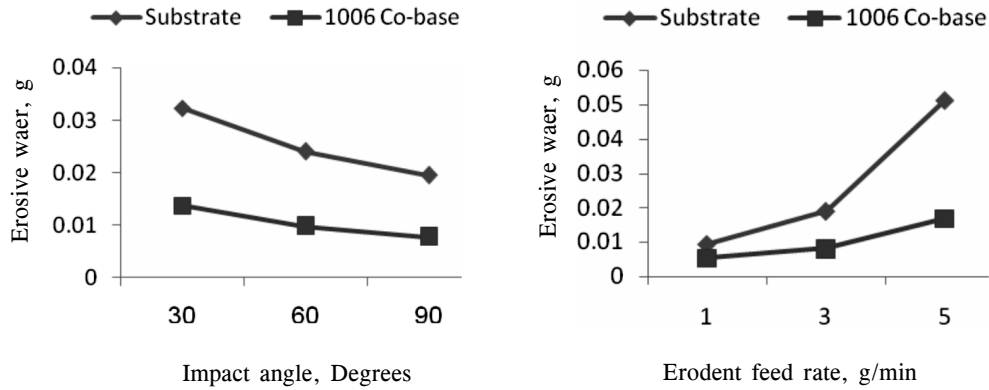
Fig. 2. Erosive wear (g) of substarte and coating as a function of (a) impact angle (degrees) and (b) erodent feed rate (g/min).

platelets are removed through ductile fracture. At high impact angle (90°), the repeated impact of the erodent causes strain hardening of the material which results in increase in strength and hardness of the coating. Further, these results in low material removal from the coating at high impact angle. There is increase in erosion wear with the increase in erodent feed rate (Fig. 2 (b)) was attributed to formations of more lips which are subsequently removed through ductile fracture [20–23].

Analysis of scanning electron microscopy (SEM) images :

Fig. 3 (a-c) shows micrographs of the worn surfaces by erosion of 1006 Co-base HVOF coatings. Cutting and platelet were the main material removal mechanisms observed in HVOF coating. At low impact angle (30°) cutting was the main material removal mechanism in this coating while at high impact angle (90°) platelets were the main material removal mechanism. At the intermediate angle (60°) both mechanisms were responsible for material removal. The extent of damage caused by each material removal mechanism determines the erosion behavior of the coatings [22–24].
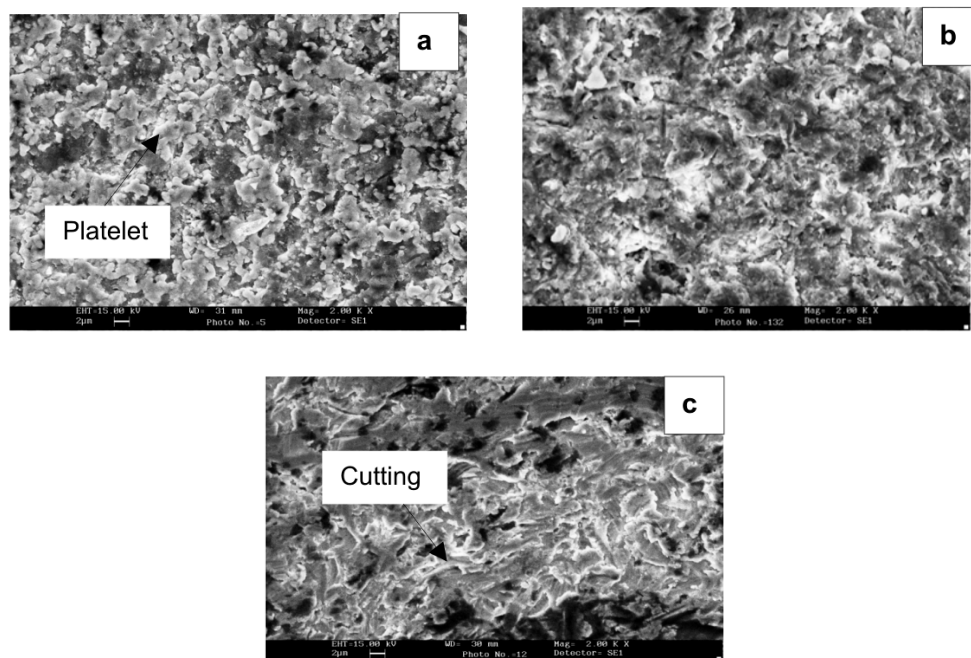
Fig. 3. Scanning electron micrograph showing the erosion behavior of 1006 Co base coating.

CONCLUSIONS

1)   The erosive wear resistance of 1006 coating is higher than the substrate. This is due to high hardness of the 1006 coating.

2)   The erosive wear decreases with the increase in impact angle.

3)   The erodent feed rate has a significant effect on the erosion wear behavior of the coating. The erosive wear increases with the increase in erodent feed rate.

4)   Cutting and platelets were the main material removal mechanisms in the 1006 Co-base coatings.

REFERENCES

1. P. Chaynes, H. N. Farmer, 758–765 (1992).

2. T. H. Kosel (Ed.), *ASM Handbook*, 18, 199 (1992)..

3. P. H. Charles Jr., *Weld. J.*, 47, (1994).

4. C. A. Mayer, *Weld. Des. Fabr.*, 61, (1982).

5. R. Arulmani and Sunil Pandey, *Journal of Indian Welding Society*, 24-34 (June 2004).

6. T. Hejwowski, S. Szewczyk and A. Weronaski, *Journal of Materials Processing Technology*, 106, 54–57 (2000).

7. P. J. Hoop and C. Allen, *Wear*, 233–235, 334–34, 1 (1999).

8. H. M. Hawthorne, B. Arsenault, J. P. Immarigeon, J. G. Legoux and V. R. Parameswaran, *Wear*, 225–229, 825–834 (1999).

9. S. B. Mishra, K. Chandra, S. Prakash and B. Venkataraman, *Surface & Coatings Technology*, 201, 1477–1487 (2006).

10. J. Kevin Stein, Brian S. Schorr and Arnold R. Marder, *Wear*, 224, 153–159 (1999).

11. J. Vicenzi, D. L. Villanova, M. D. Lima, A. S. Takimi, C. M. Marques and C. P. Bergmann, *Materials and Design*, 27, 236–242 (2006).

12. Hazoor Singh Sidhu, Buta Singh Sidhu and S. Prakash, *Surface & Coatings Technology*, 202, 232–238 (2007).

13. S. P. Sharma, D. K. Dwivedi and P. K. Jain, Proceedings of the Institution of Mechanical Engineering, Part J- Journal of Engineering Tribology, 222, 925–33 (2008).

14. S. P. Sharma, D. K. Dwivedi and P. K. Jain, *Wear*, 267, 853–859 (2009).

15. H. R. Shetty, T. H. Kosel and N. F. Fiore, *Wear*, 80, 347–376 (1982).

16. J. Saaedi, T. W. Coyle, S. Mirdamadi, H. Arabi and J. Mostaghimi, *Surface & Coatings Technology*, 202, 5804–5811 (2008).

17. A. R. Marder, "ASM Handbook, Material selection and design", ASM International, Materials park, Ohio, 20, pp. 470–490 (1997).

18. M. Vite, M. Castillo, L. H. Hernandez, G. Villa, I. H. Cruz and D. Stephane, *Wear*, Vol. 258, pp. 70–76 (2005).

19. J. L. Otterloo, Van De Mol and J. Hossont, De M. TH., *Acta Materialia*, 45, 1225–1236 (1997).

20. J. G. A. Bitter, *Wear*, 6, 5–21, (1963).

21. J. G. A. Bitter, *Wear*, 6, 169–190, (1963).

22. I. Finnie, J. Wolak and Y. Kabil, *ASTM J. Material*, 2, 682–700, (1967).

23. G. P. Tilly and W. Sage, *Wear*, 16, 447–465, (1970).

24. A. J. Ninham and A. V. Lev, *Wear*, 121, 325–346, (1998).